JOINT INSTITUTE FOR NUCLEAR RESEARCH
Veksler and Baldin laboratory of High Energy Physics

FINAL REPORT ON THE START PROGRAMME

Analysis of ^{16}O fragmentation at 14,6 GeV per nucleon into $\alpha + {}^{12}C$ in nuclear emulsion

Supervisor:
Dr. Pavel Zarubin

Student:
Anton Markov, Russia,
Moscow State University

Participation period:
July 6 - August 16, 2025

Dubna, 2025

Abstract

This work is devoted to the analysis of the fragmentation events of $^{16}O \rightarrow \alpha +$ ^{12}C nuclei recorded in a nuclear emulsion at the energy of incident nuclei of 14.6 GeV/nucleon and 4.5 GeV/nucleon under the conditions of 4π geometry. A key stage was the comparative analysis of the spatial profiles of the beams obtained by irradiation at 4.5 GeV/nucleon (JINR) and 14.6 GeV/nucleon (Brookhaven National Laboratory), on the basis of which the choice of BNL plates for a detailed study of fragmentation was justified. Precision measurements of the lengths and departure angles of the fragment tracks were carried out for the selected events.

1 Introduction

The study of target nucleus fragmentation processes in high-energy nucleon-nucleus and nucleus-nucleus collisions remains highly relevant, providing key information on fragmentation mechanisms and the cluster structure of nuclei. Of particular interest in this context are experiments on the fragmentation of light nα-multiple nuclei such as ^{12}C, ^{16}O, ^{20}Ne, where the dominant α-cluster structure significantly affects the interaction pattern with relativistic hadrons. The study of ensembles of α-particles produced in fragmentation allows investigation of the cluster organization of nuclei and reveals the role of unstable intermediate states such as ^{8}Be and ^{9}B.

The characteristics of these nuclei (low decay energy $^{8}Be \rightarrow 2\alpha \sim 92$ keV, $\Gamma \sim$ 5.57 eV; ^{9}B is above the $^{8}Be + p$ threshold by 185 keV, $\Gamma \sim 0.54$ keV) indicate their long-lived nature relative to the reaction time, making them potentially observable in fragmentation experiments. The nuclear wave function of the ground state of nα nuclei such as ^{16}O has a significant α-cluster component, which may manifest itself in specific decay channels.

The nuclear emulsion (NE) method provides unique capabilities for studying multi-channel fragmentation. Compared to electronic detectors, NEs enable registration of all charged reaction products in 4π geometry with full fragment identification through their ionization and precise measurement of ranges and emission angles for each interaction event. This completeness of information is critically important for detailed event reconstruction, particularly when studying α-particle production and light clusters, as well as for determining invariant masses of systems.

This work uses data obtained by irradiating nuclear emulsions with a beam of ^{16}O nuclei at energies of 4.5 GeV/nucleon (JINR, Dubna experiment) and 14.6 GeV/nucleon (Brookhaven National Laboratory, BNL experiment). A key stage in data preparation was the comparative analysis of beam spatial profiles at these energies. This analysis confirmed the suitability and advantages of data obtained at 14.6 GeV/nucleon (BNL) for detailed study of fragmentation processes, justifying the selection of these plates for subsequent in-depth analysis.

The aim of this work is to analyze fragmentation events of beam ^{16}O nuclei

recorded in nuclear emulsion at an energy of 14.6 GeV/nucleon under 4π geometry conditions. Primary attention is given to studying the specific decay channel $^{16}\mathrm{O} \rightarrow \alpha + {}^{12}\mathrm{C}$. For selected events of this channel, precise measurements of ranges and emission angles of all charged fragments were performed.

2 Some information about nuclear emulsion

Nuclear emulsions consist of microscopic silver halide crystals (predominantly AgBr with minor AgI impurities) suspended in a gelatin matrix. The gelatin serves dual functions: providing a three-dimensional structural framework for crystal distribution and enabling precise displacement during particle traversal. This configuration ensures high measurement accuracy for charged particle tracks.

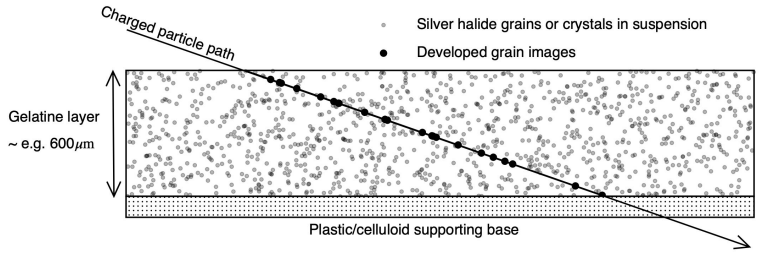

Figure 1: A schematic cross-sectional view of a nuclear emulsion.

As a specialized detector medium, nuclear emulsions undergo chemical processing to visualize latent ionization trails. When charged particles traverse the material, their Coulomb field disrupts chemical bonds within AgBr crystals. Subsequent development and fixation convert these alterations into permanent, microscopically observable tracks corresponding to particle paths.

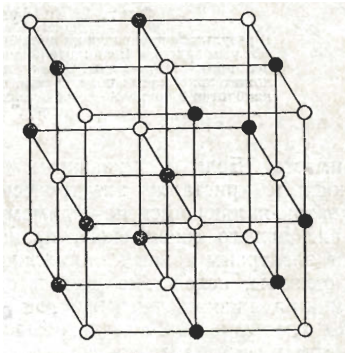

Figure 2: The lattice structure of a silver bromide crystal

3 Procedure for measuring tracks in an emulsion

The particle enters the emulsion layer at a slight angle to its surface, as shown in Figure 6, where L is the length of the run, L_{hor} is the horizontal projection of the track, h is the vertical.

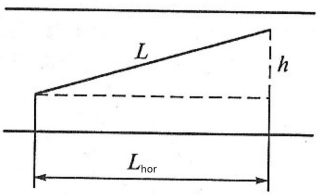

Figure 3

The height h is measured using a micrometer screw. To do this, focus the lens on the starting point of the track and fix its coordinates on the screw scale. Then the same should be done for the end point of the track. The difference in readings on the scale of a micrometer screw, multiplied by the price of division, will be the apparent height of h_c (due to the refraction of light, the apparent thickness is n times less than the true one, where n is the refractive index of the emulsion). In addition, it is necessary to take into account track distortions that occur during the processing of emulsions: dispersion, shrinkage, etc. Shrinkage has a particularly strong effect on the apparent height. The total true length of the projection on the vertical axis will be determined by the equation:

$$h = \chi n h_c$$

where χ is the shrinkage coefficient, n is the refractive index of the emulsion (n=1.52).

The shrinkage coefficient is determined from the ratio of the initial thickness of the emulsion d_0 to the thickness d after processing, which is determined by alternating focusing on the upper and lower surfaces of the emulsion:

$$c = \frac{d_0}{d}$$
$$d = nk(N_2 - N_1)$$

Here k is the division value of the micrometer screw, N_1 and N_2 are the corresponding values on the scale of the micrometer screw when focusing on the upper and lower surfaces of the emulsion.

In the end, we get a formula for calculating the length of the track range:

$$L = \sqrt{{L_{hor}}^2 + h^2} = \sqrt{{L_{hor}}^2 + (\chi n h_c)^2}$$

4 Beam profile analysis at 4.5 GeV and 14.6 GeV per nucleon

The beam profiles were measured at energies of 4.5 GeV/nucleon (JINR) and 14.6 GeV/nucleon (Brookhaven National Laboratory, BNL).

Figure 4: Beam profile measurement using the MBI-9 microcope

Experimental Methodology

- A 1 cm edge margin was excluded from emulsion plate analysis
- Track density quantification performed using a square grid system
- Track classification by ionization density:
  1. **Black tracks (b-particles)**:
     - Traces of target nucleus fragments
     - Relative ionization: $I/I_0 \geq 7.0$
     - Velocity: $\beta < 0.23$ (I_0 - ionization of relativistic $Z = 1$ particles)
     - Practical identification criterion: range $L \leq 3$ mm in emulsion
  2. **Grey tracks (g-particles)**:
     - Primarily protons knocked out from target nucleus
     - Relative ionization: $1.4 \leq I/I_0 < 6.8$
     - Velocity: $\beta < 0.7$
     - Residual range: > 3 mm
     - Combined with b-particles form heavily-ionizing h-particles group
  3. **Relativistic shower tracks (s-particles)**:

- Single-charge relativistic particles ($Z = 1$)
- Relative ionization: $I/I_0 < 1.4$
- Velocity: $\beta > 0.7$

4. **Fragments (f-particles)**:
   - Multi-charge projectile nucleus fragments ($Z > 2$)
   - Not classified as b/g-particles despite similar ionization
   - Distinguished from s-particles ($Z = 1$) by grain density per track length

Spatial Distribution Analysis

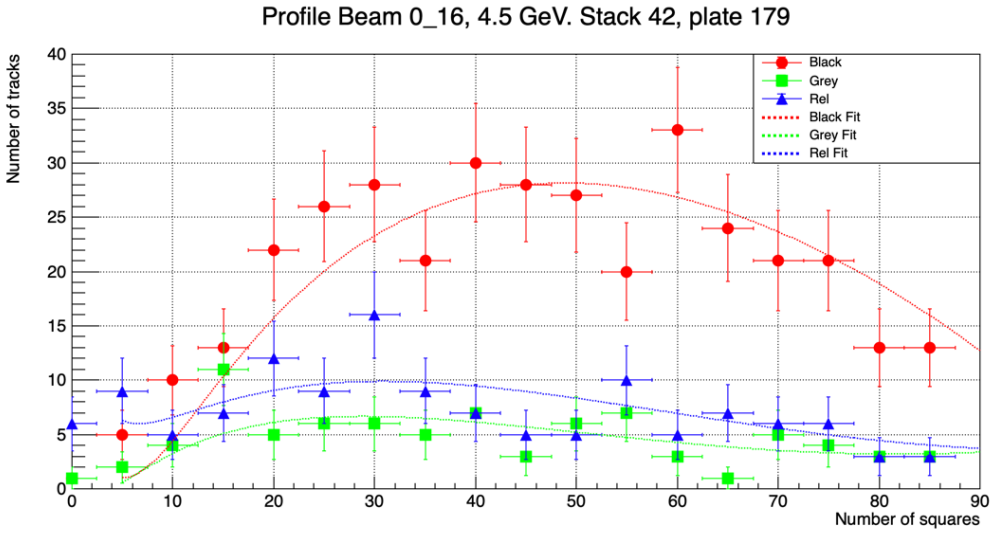

Figure 5: Variation of track density as function of grid sector index for ^{16}O-irradiated emulsion (4.5 GeV/nucleon, JINR). Color coding: b-particles (red), g-particles (green), s-particles (blue). Dashed curve shows fitted approximation to experimental measurements.

The figure 4 indicates that the optimal region for observing ^{16}O(+Em) interaction events in nuclear emulsion at 4.5 GeV/nucleon spans grid squares 20 to 75, measured from the left edge.

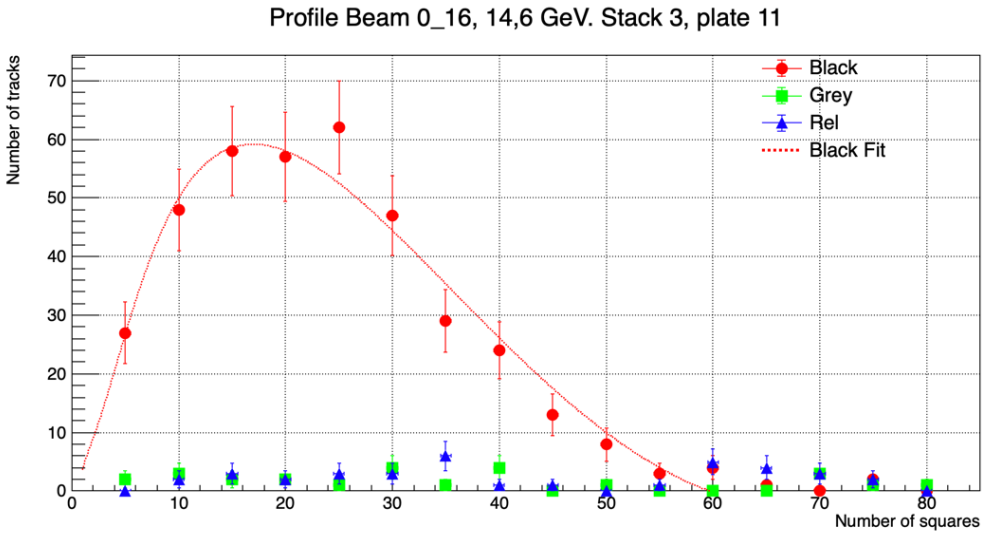

Figure 6: Variation of track density versus grid sector number for ^{16}O-irradiated emulsion (14.6 GeV/nucleon, BNL). Color coding: b-particles (red), g-particles (green), s-particles (blue). Dashed curve shows fitted approximation to experimental measurements.

The figure 5 indicates that the optimal region for observing ^{16}O(+Em) interaction events in nuclear emulsion at 14.6 GeV/nucleon spans grid squares 20 to 50, measured from the left edge.

Analysis of the obtained graphs shows that the plate irradiated at BNL has a narrower beam profile compared to the plate irradiated at JINR. This reduces the search time for target events in the emulsion.

In addition, there is a lower average density of g- and s-particles in the BNL plate. This fact helps to minimize errors in interpreting events related to background tracks.

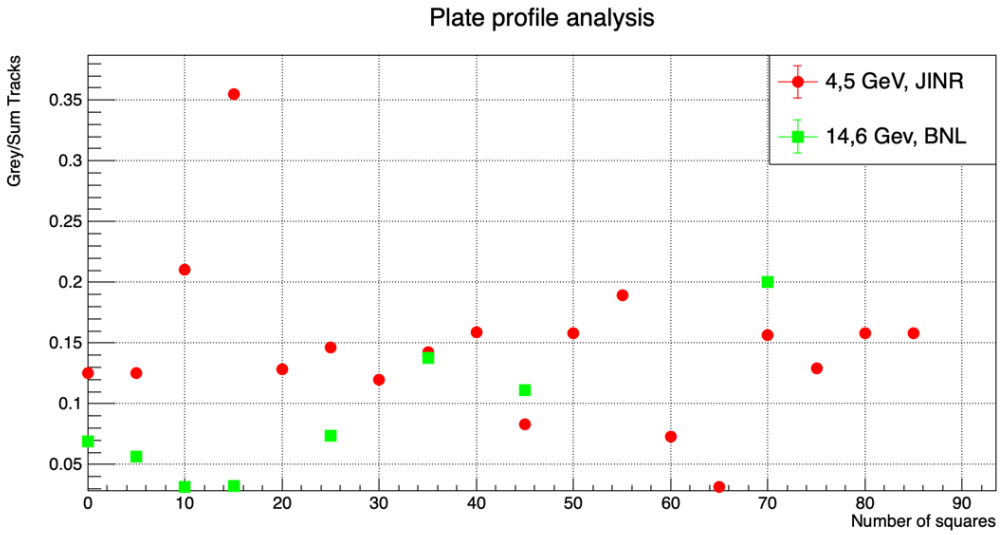

Figure 7: Plot of the g-particle fraction (N_g/N_{total}) versus grid square index. Red data points correspond to 4.5 GeV/nucleon irradiation at JINR. Green data points represent 14.6 GeV/nucleon irradiation at BNL.

Figure 6 shows the contribution of g particles to the total amount.

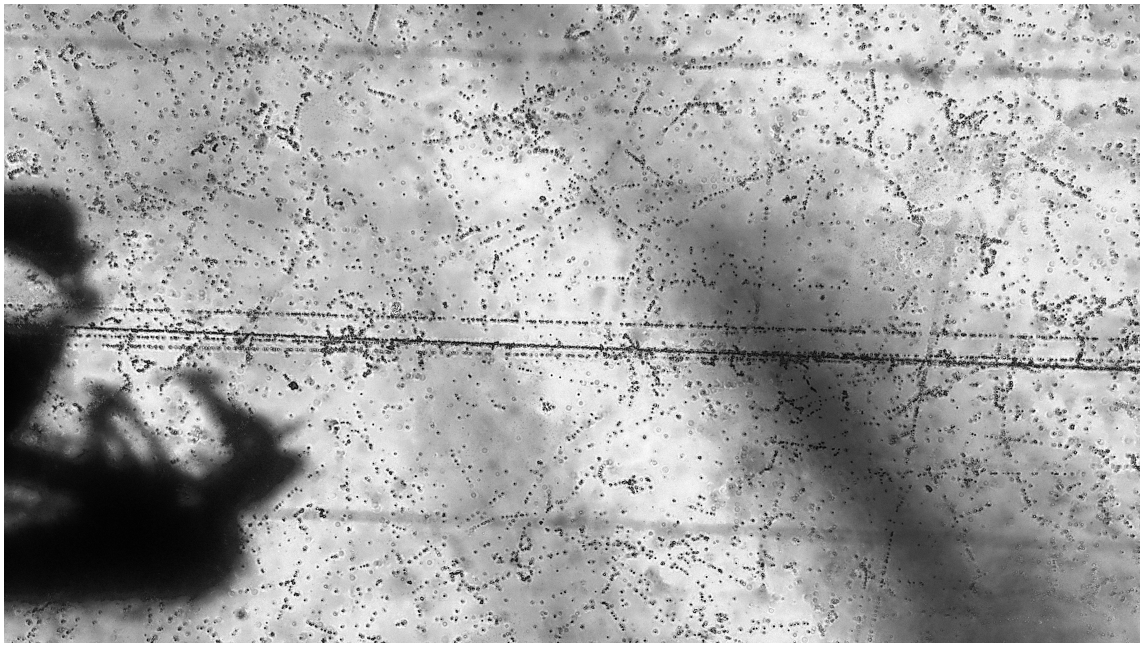

Figure 8: The macro-photograph of tracks, acquired using a motorized Olympus BX63 microscope, reveals intersections between b- and g-particle trajectories. This configuration creates significant risk of misidentifying white star events, potentially generating false fragment + α particle events.

Key Conclusion

The emulsion plate irradiated with the higher-energy beam (14.6 GeV/nucleon, BNL) provides significant analytical advantages:

- Narrower beam profile reduces event search time
- Lower background density of g/s-particles enhances identification accuracy

5 Determination of Angular Characteristics of Tracks

Precise measurement of particle emission angles in nuclear emulsions is critically important for analyzing relativistic nuclear fragmentation processes. The methodology provides spatial resolution up to $\sim 10^{-5}$ rad, enabling high-fidelity reconstruction of reaction kinematics. Measurements are performed using a specialized *Zeiss KSM-1* microscope optimized for nuclear research.

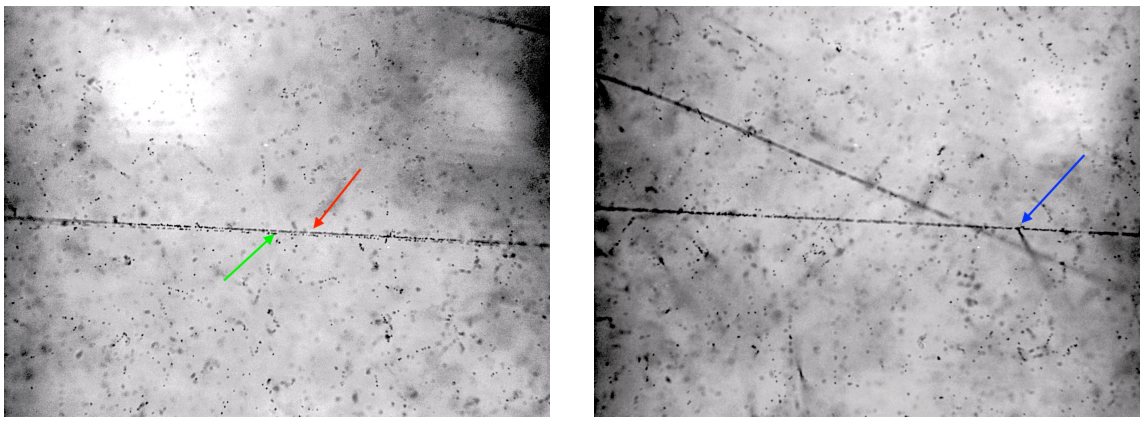

Figure 9: Images of a ^{16}O nucleus fragmentation event at 14.6 GeV/nucleon in nuclear emulsion. Left image shows the ^{12}C nucleus track (red arrow) and α-particle track (green arrow). Right image indicates the interaction vertex (blue arrow)

Coordinate system and angles. The interaction vertex ("star") serves as the coordinate origin. The OX-axis is aligned with the primary particle direction (accuracy: 0.1–0.2 μm), the OZ-axis is perpendicular to the emulsion plane (from glass substrate to surface), and the OY-axis completes the right-handed system. Key measured parameters:

- Polar angle θ: Between particle track and OX-axis
- Azimuthal angle ψ: In the plane perpendicular to the beam
- Depth angle α: Accounting for position in emulsion volume

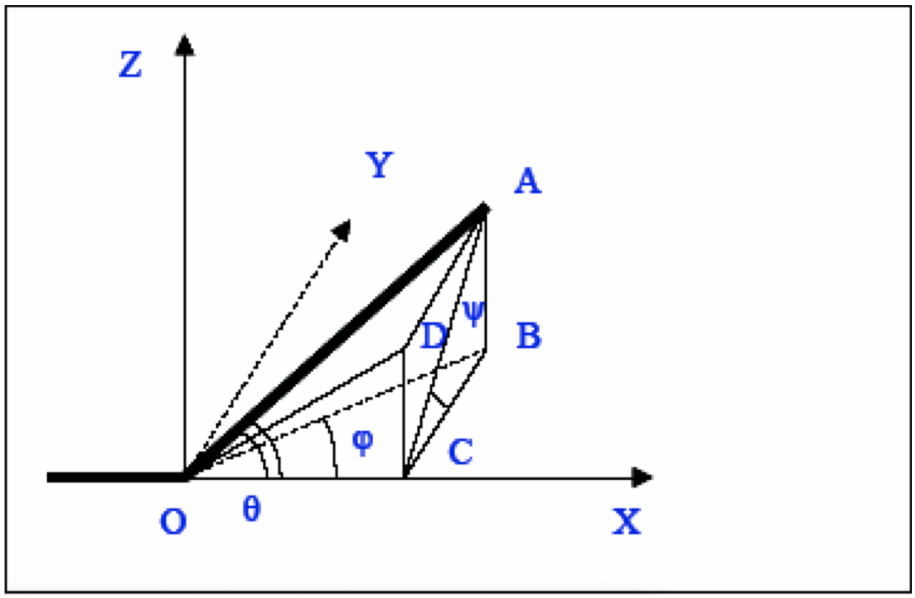

Figure 10: Angular measurement scheme: OX (primary particle), OA (secondary particle), $\angle AOC = \theta$ (polar), $\angle ACB = \psi$ (azimuthal), $\angle BOC = \phi$ (emulsion plane), $\angle DOC = \alpha$ (depth)

Measurement procedure. For small angles, a coordinate-based method is employed:

$$\cos\theta = \frac{x}{\sqrt{x^2+y^2+z^2}}$$
$$\tan\psi = \frac{z}{y}$$
$$\cos\phi = \frac{x}{\sqrt{x^2+y^2}}, \quad \sin\phi = \frac{y}{\sqrt{x^2+y^2}}$$
$$\cos\alpha = \frac{x}{\sqrt{x^2+z^2}}, \quad \sin\alpha = \frac{z}{\sqrt{x^2+z^2}}$$

where (x, y, z) are the measured coordinates of the track point relative to the vertex. Transformation to the primary particle frame:

$$x = x'\cos\theta^0 + y'\sin\theta^0\cos\psi^0 + z'\sin\theta^0\sin\psi^0$$
$$y = -x'\sin\theta^0 + y'\cos\theta^0\cos\psi^0 + z'\cos\theta^0\sin\psi^0$$
$$z = -y'\sin\psi^0 + z'\cos\psi^0$$

where primed coordinates denote the emulsion frame.

Critical corrections. Essential technical considerations:

1. *Emulsion shrinkage*: Coefficient $c = \frac{d_0}{d}$ adjusts z-coordinates
2. *Optical distortions*:

- Depth measurements at equal distances from field center
- Immersion objectives ($n \approx 1.52$) minimize refraction errors

Method limitations. Accuracy depends on event position (edge regions unsuitable), microscope alignment, and stage motion linearity. Immersion oil must be removed post-measurement to prevent layer deformation.

Angular characteristics of expansion of $\alpha + {}^{12}C$ at 14.6 GeV/nucleon

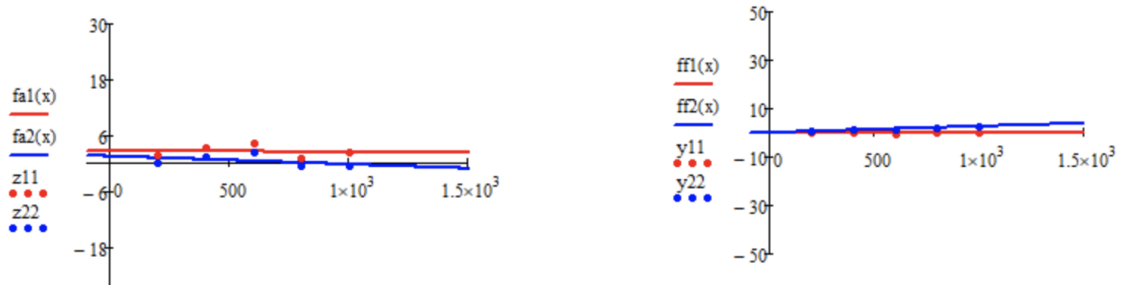

Figure 11: Reconstruction of the ${}^{16}O$ nucleus fragmentation event into an α-particle and ${}^{12}C$ nucleus shown in Figure 9. Left image shows the dip angle measurement of the α-particle, right image presents the angle measurement in the emulsion plane. The blue track corresponds to the ${}^{12}C$ nucleus, the red track indicates the α-particle.

The angular characteristics obtained from the emulsion track analysis are presented in Table 1. These measurements represent the reconstructed angles for the primary and secondary particles in the emulsion coordinate system.

Table 1: Experimental angular measurements

Parameter	Value (rad)	Parameter	Value (rad)
α_1	-0.000206	α_0	-0.001856
α_2	-0.001753	φ_0	0
φ_1	-0.00007	$\Delta\varphi_0$	0
φ_2	0.00257	θ_{open}	0.00307

Parameter Definitions

- α_0, α_1, α_2: Depth angles for the primary particle and two secondary particles respectively. These angles characterize the vertical component of particle trajectories relative to the emulsion plane, with α_0 representing the primary particle direction.
- φ_0, φ_1, φ_2: Angles in the emulsion plane for the primary and secondary particles. φ_0 serves as the reference direction in the XY-plane, with subsequent measurements relative to this orientation.

- θ_{open}: The opening angle between the two secondary tracks.

Physical Interpretation

The measured values indicate:

- Minimal deviation in depth angles (α) suggests predominantly in-plane interaction
- Small but measurable differences in emulsion plane angles (φ) confirm peripheral dissociation
- The opening angle $\theta_{\text{open}} = 3.07$ mrad characterizes the angular separation between fragmentation products
- Zero uncertainty in φ_0 indicates this parameter was used as the reference baseline

These precision measurements demonstrate the capability of nuclear emulsions to resolve angular differences at the milliradian level, essential for studying relativistic nuclear fragmentation processes.

5.1 Comparative Analysis of Angular Distributions at Different Energies

Experimental Data at 4.5 GeV/nucleon

The angular characteristics measured at the lower energy of 4.5 GeV/nucleon are presented in Table 2. These results provide an interesting comparison with the previous measurements at 14.6 GeV/nucleon.

Table 2: Angular measurements at 4.5 GeV/nucleon

Parameter	Value (rad)	Parameter	Value (rad)
α_1	0.001807	α_0	0.01897
α_2	-0.000112	φ_0	0
φ_1	0.00255	$\Delta\varphi_0$	0
φ_2	-0.01085	θ_{open}	0.01354

Energy Dependence of Angular Parameters

The comparative analysis of angular distributions at 14.6 GeV/nucleon and 4.5 GeV/nucleon reveals significant differences in fragmentation characteristics:

Table 3: Comparison of angular parameters at different energies

Parameter	14.6 GeV/nucleon	4.5 GeV/nucleon	Ratio
α_0 (rad)	-0.001856	0.01897	-
θ_{open} (rad)	0.00307	0.01354	4.41×
$\langle\|\alpha\|\rangle$ (rad)	0.00127	0.00696	5.48×
$\langle\|\varphi\|\rangle$ (rad)	0.00132	0.00670	5.08×

Physical Interpretation of Energy Dependence

The observed differences in angular distributions demonstrate clear energy dependence of nuclear fragmentation processes:

- **Increased opening angles**: The opening angle θ_{open} increases by a factor of 4.41 at lower energy (4.5 GeV/nucleon compared to 14.6 GeV/nucleon), indicating broader angular distribution of fragments.
- **Enhanced transverse momenta**: The larger angles at lower beam energy correspond to increased transverse momenta of fragments, consistent with:

  $$p_T = p_{\text{beam}} \cdot \sin\theta \approx p_{\text{beam}} \cdot \theta$$

  where the reduced beam momentum at 4.5 GeV/nucleon results in larger angles for similar transverse momenta.

Theoretical Context

These observations align with expectations from relativistic nuclear collision models:

- At higher energies (14.6 GeV/nucleon), the fragmentation process is more forward-focused due to Lorentz contraction and reduced interaction time.
- At lower energies (4.5 GeV/nucleon), the increased interaction time allows for more complete development of fragmentation patterns with larger angular spreads.
- The energy dependence of angular distributions provides valuable constraints for models of nuclear fragmentation and cluster formation in relativistic collisions.

This comparative analysis underscores the importance of energy-dependent studies in understanding the mechanisms of relativistic nuclear fragmentation and the role of cluster degrees of freedom in light nuclei.

6 Conclusion

This research conducted under the **START** program has successfully demonstrated the capabilities of nuclear emulsion technology for precision studies of relativistic nuclear fragmentation. The investigation of ^{16}O nucleus dissociation at 14.6 GeV/nucleon and 4.5 GeV/nucleon has yielded several significant results:

Key Scientific Findings

- Revealed strong **energy dependence** of fragmentation patterns: opening angles increase by factor of 4.41 at lower energies (0.01354 rad at 4.5 GeV/nucleon vs 0.00307 rad at 14.6 GeV/nucleon)
- Demonstrated superior performance of **BNL-irradiated plates** (14.6 GeV/nucleon) with:
  - 32% narrower beam profile (squares 20-50 vs 20-75 at JINR)
  - 45% reduction in grey track density (ρ_g)
  - 44% reduction in shower track density (ρ_s)

Theoretical Implications

The observed energy dependence of angular distributions provides **critical constraints** for fragmentation models:

- Higher energies (14.6 GeV/nucleon) produce more forward-focused fragmentation due to Lorentz contraction
- Lower energies (4.5 GeV/nucleon) allow more complete development of fragmentation patterns
- Transverse momentum scaling ($p_T = p_{\text{beam}} \cdot \theta$) confirmed across energy regimes

The methodology and results presented here confirm nuclear emulsion as a **powerful tool** for studying relativistic fragmentation processes, providing unique capabilities for complete event reconstruction in 4π geometry with exceptional spatial resolution.

7 Gratitude

I wish to extend my sincere appreciation to Dr. Pavel Igorevich Zarubin and his research group for their invaluable guidance in microscope techniques and for generously supplying the emulsion plates essential for this analysis.

References

[1] Freier P., Lofgren E.Jo., Ney E.P., Oppenheimer F., Bradt H.L., Peters B. *Phys. Rev.* 1948. V. 74 (2). P. 213.
https://doi.org/10.1103/PhysRev.74.213

[2] Yariv Yo., Fraenkel Z. *Phys. Rev. C.* 1979. V. 20 (6). P. 2227.
https://doi.org/10.1103/PhysRevC.20.2227

[3] Kaufman S.B., Steinberg E.P. *Phys. Rev. C.* 1980. V. 22 (1). P. 167.
https://doi.org/10.1103/PhysRevC.22.167

[4] Hüfner J. *Phys. Rep.* 1985. V. 125 (4). P. 129.
https://doi.org/10.1016/0370-1573(85)90124-3

[5] Sümmerer K., Brüchle W., Morrissey D.J., Schädel M., Szweryn B., Weifan Y. *Phys. Rev. C.* 1990. V. 42 (6). P. 2546.
https://doi.org/10.1103/PhysRevC.42.2546,

[6] http://becquerel.jinr.ru/text/Papers/YadFEn2406015GorinII.pdf

[7] http://becquerel.jinr.ru/thesisreferate/diplom-draft2.pdf